



## The Weld Heat-Affected Zone of the 18Ni Maraging Steels

Ghost boundary networks visible in the heat-affected zone are attributed to constitutional liquation of titanium sulfide inclusions to produce a solute-rich liquid which penetrates the grain boundaries

BY J. J. PEPE AND W. F. SAVAGE

**ABSTRACT.** A recent investigation of the weld heat-affected zone of the 18 Ni maraging steels revealed that "constitutional liquation" of titanium sulfide is responsible for the formation of a liquid grain boundary film; this drastically reduces the resistance of these steels to heat-affected zone hot cracking.

In addition, continued investigations of the weld heat-affected zone of the 18 Ni maraging steels revealed that an anomalous grain size distribution was present immediately adjacent the weld fusion line. It was observed that the grain size immediately adjacent the fusion line was smaller than the grain size further removed from the fusion line. High-speed high-temperature tests on the 18 Ni maraging steels have clearly shown that this anomalous grain size distribution results from the interaction of solute-rich liquid pools, produced by "constitutional liquation" of titanium sulfide inclusions, with a moving grain boundary network.

This investigation also revealed that ghost boundary networks visible in the weld heat-affected zone are attributed to "constitutional liquation" of titanium sulfide inclusions to produce a solute-rich liquid which penetrates the grain boundaries. A schematic representation is pre-

sented together with actual metallographic data illustrating the origin of the ghost boundary network in the 18 Ni maraging steels.

### Introduction

A recent investigation<sup>1</sup> of the weld heat-affected zone of the 18Ni maraging steels has shown that a liquid grain-boundary film is formed at temperatures significantly below the bulk solidus of the alloy; the film is formed by the interaction of moving grain boundaries and solute-rich liquid pools formed by "constitutional liquation" of titanium-sulfide inclusions. It was also shown that the presence of these solute-rich liquid grain-boundary films drastically reduce the resistance of the 18Ni maraging steels to heat-affected zone hot cracking.

In addition, continued investigations of the weld heat-affected zone of the 18Ni maraging steels revealed that "constitutional liquation" was responsible for other microstructural features in this region of the weld. It is the purpose of this paper to point out these additional findings.

### Materials and Experimental Work

The two heats of 18 Ni maraging steel used in this investigation were prepared by conventional mill practice. One heat (heat X53674) was obtained from the U.S. Steel Corpora-

tion in the form of  $1/16$  in. thick sheet. The other heat was obtained from the International Nickel Company in the form of  $1/2$  in. thick plate. The ladle analysis and room temperature mechanical properties of the aged materials are listed in Tables 1 and 2, respectively.

### Weldment Studies

A gas tungsten-arc weld bead on  $1/2$  in. thick plate was made by standard techniques using the following welding conditions: 320 amp, 9 v and 3 ipm arc travel speed.

### Gleeble Studies

The  $1/2$  in. by 3 in. specimens used in the Gleeble studies were sheared from hot-rolled  $1/16$  in. thick sheet material. A 0.252 in. diameter hole was made near each end of the specimen to accommodate 0.250 in. locator pins used to prevent slippage in the extended jaws of the Gleeble.

All specimens were rapidly heated to elevated temperatures following a linear thermal cycle in a specially designed argon-atmosphere box (shown schematically in Fig. 1) to limit surface oxidation. The extended jaws of the Gleeble, made from  $1 1/4$  in. RWMA Class 2 electrode stock, entered the atmosphere box through a  $1 1/4$  in. diameter "O" ring seal at either end of the atmosphere box as shown in Fig. 1.

A specially designed water-

J. J. PEPE is Senior Project Metallurgist, Maggs Research Center, Watervliet Arsenal, Watervliet, N. Y. and W. F. SAVAGE is Director of Welding Research Dept. of Material Engineering, Rensselaer Polytechnic Institute, Troy, N. Y.

Paper presented at the AWS National Fall Meeting held in Houston, Texas on October 2-5, 1967.

**Table 1—Ladle Analysis of Two Heats of 18 Ni Maraging Steel, %**

Heat no.	C	Mn	P	S	Si	Ni	Co	Mo	Al	Ti	Ca
X5674	0.02	0.04	0.005	0.010	0.20	17.86	8.04	4.89	0.11	0.39	<sup>a</sup>
<sup>a</sup>	0.016	0.07	0.005	0.024	0.11	18.13	7.73	4.60	0.10	0.36	0.017

<sup>a</sup> Not available.

**Table 2—Room Temperature Mechanical Properties of Two Heats of 18 Ni Maraging Steel**

Heat no.	Test direction	Ultimate tensile strength, psi	0.2% yield strength, psi	Elongation in 2 in., %	Reduction in area, %
X53674	Longitudinal	268,000	258,000	5	<sup>b</sup>
X53674	Transverse	271,000	266,000	3	51.3
—	<sup>a</sup>	257,000	246,000	11.5	51.3

<sup>a</sup> Not given.

<sup>b</sup> Not determined.

quenching fixture located within the atmosphere box permitted quenching rates exceeding 25,000° F/sec to be obtained at the specimen surface. Actuation of a microswitch, at any preselected time in the thermal cycle, caused a solenoid valve to open, applying 100 psi compressed air to force the water from a holding reservoir to the surface of the specimen.

#### Metallographic Studies

Suitably polished surface were obtained by conventional metallographic techniques consisting of sectioning, mounting in an epoxy resin, and mechanically polishing through Linde "B".

### Results and Discussion

#### Anomalous Grain Size Distribution

In the course of this investigation it was noted that the average grain size in the region of the heat-affected zone immediately adjacent to the fusion line appeared to be smaller than that

at a greater distance from the fusion line. Accordingly, a statistical determination of the average grain size near the fusion line of the gas tungsten arc bead on 1/2 in. plate was performed at 500X magnification, both for grains in the heat-affected zone which intersected the fusion line and for grains which intersected a line paralleling the fusion line at a perpendicular distance of 0.004 in. (2 in. at 500X).

Based upon the intercept method, the average diameter of the grains located at a distance of 0.004 in. from the fusion line was found to be 0.00214 in. By comparison, the average diameter of the grains intersecting the fusion line was only 0.00188 in. These data are inconsistent with predictions based upon normal grain-growth behavior.

It should be recognized that both the peak temperature and the integrated time at temperature, experienced by a point in the heat-affected

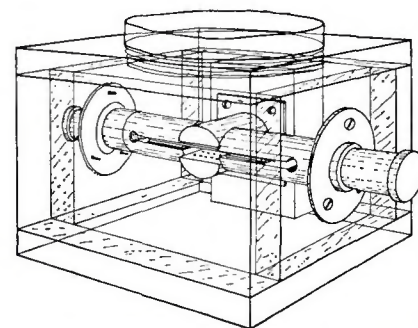


Fig. 1—Schematic diagram of argon atmosphere box

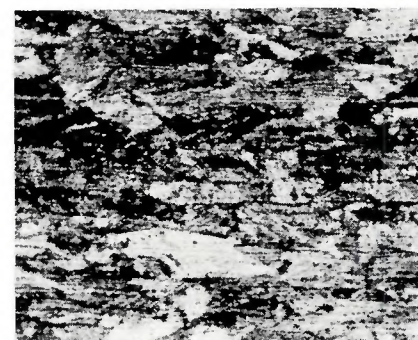


Fig. 2—Microstructure of a transverse section of the as-received material. 10% chromic acid electrolytic etch followed by 10% ferric chloride etch. X100 (reduced 46% on reproduction)

zone, increase continuously as the distance from the fusion line is diminished. Therefore, if normal grain-growth behavior were experienced, the grain diameter should increase continuously as the distance from the fusion line diminishes. Since the grain size data reported above show a reversal of this trend, it is obvious that some competing reaction must be present which inhibits grain growth near the weld fusion line. Accordingly, an investigation was undertaken to determine the mechanism responsible

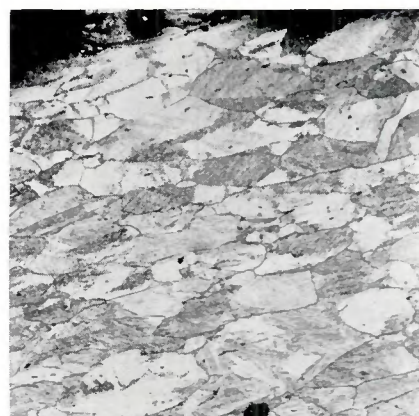


Fig. 3—Microstructure produced in as-received material heated at 1000° F/sec to 900° F and immediately water quenched. 10% chromic acid electrolytic etch followed by 10% ferric chloride etch. X100 (reduced 28% on reproduction)



Fig. 4—Microstructure produced in as-received material heated at 1000° F/sec to 1350° F and immediately water quenched. 10% chromic acid electrolytic etch followed by 10% ferric chloride etch. X100 (reduced 28% on reproduction)



Fig. 5—Microstructure produced in as-received material heated at 1000° F/sec to 1800° F and immediately water quenched. 10% chromic acid electrolytic etch followed by 10% ferric chloride etch. X100 (reduced 28% on reproduction)

for this anomalous grain-size distribution.

### Gleeble Studies

**Rapid Heating to Peak Temperature.** As an initial step in investigating the anomalous grain-size distribution observed near the weld fusion line of the gas tungsten-arc weldment made on an 18 Ni maraging steel, a study was made of the metallurgical changes produced during rapid heating of these steels. A series of specimens, machined from the  $1/16$  in. thick as-received sheet, were heated to different peak temperatures in the range 700 to 2200° F in the Gleeble at a controlled rate of 1000° F/sec. Immediately upon reaching peak temperature, each sample was water quenched at a rate in excess of 25,000° F/sec to preserve the grain size present at the elevated temperature.

Figure 2 is a photomicrograph at X100 magnification of a cross section taken normal to the sheet surface and parallel to the final rolling direction. This microstructure is typical of that of the as-received 18 Ni maraging steel, as revealed by a chromic-acid electrolytic etch followed by a ferric-chloride etch. Note that the grain structure of this specimen is elongated in the same general direction as the alternating light and dark etching bands. This indicates that the final rolling operation introduced a small amount of cold work.

Careful examination of this sample revealed a number of dark, rod-like inclusions, oriented parallel to the banding present and located both at grain boundaries and within the matrix of the grain.

Figures 3-5 are photomicrographs taken at X100 magnification of similar cross sections in Gleeble specimens heated at 1000° F/sec to 900, 1350 and 1800° F, respectively, and immediately quenched to room temperature. The etching procedure used for these and all subsequent specimens in this series was identical to that discussed in connection with Fig. 2, unless otherwise specified.

Examination of Figs. 3-5 reveals that no significant metallographic changes occurred until a peak temperature of 1800° F was reached. At this temperature (see Fig. 5) a considerable number of small equiaxed grains are evident in the vicinity of triple points between the original elongated grains. Since the  $\alpha$ - $\gamma$  transformation temperature for the 18 Ni maraging steels is reported to be approximately 1300° F for heating rates of 800° F/sec and to decrease with increasing heating rates<sup>2</sup> the samples must have experienced a crystallographically re-

versible transformation. In other words, the transformations from martensite to austenite on heating, and from austenite to martensite on cooling, must have occurred with experiencing either a change in grain size or migration of the grain boundaries. This would explain the apparent stability of the elongated grain structure and is consistent with the fact that the  $\alpha$ - $\gamma$  transformation is reported<sup>2</sup> to be a crystallographically reversible shear process.

Figure 6 is a photomicrograph at X100 magnification of a similar specimen heated at 1000° F/sec to 2200° F and immediately water quenched. The fine equiaxed grains indicate that complete recrystallization occurred by the time the peak temperature reached 2200° F. Note that many of the grain boundaries are pinned by inclusions, but that the grain boundaries cross through the horizontal segregation bands except for the rather pronounced band near the center of Fig. 6.

The above investigation of the recrystallization behavior was conducted at a constant heating rate of 1000° F/sec. However, in the following portion of the study, the time to reach peak temperature was maintained constant instead of the heating rate. This procedure is more convenient to program on the Gleeble and thus the heating time for the balance of the specimens was maintained constant at 2.2 sec, the time required to reach 2200° F in the specimen shown in Fig. 6.

Figure 7 is a photomicrograph at X100 magnification showing the structure formed by rapid heating to 2350° F and immediately quenching to room temperature. The grain structure is equiaxed and the grain size appears to be approximately identical to that formed by rapid heating to 2200° F (see Fig. 6). Again note that many of the grain boundaries appear to be pinned by inclusions.

The first evidence of "constitutional liquation" is seen in Fig. 8 which is a photomicrograph at X100 magnification of a specimen rapidly heated to 2400° F and immediately water quenched to room temperature. Note the numerous circular to elliptical-shaped features scattered throughout the field of view with an internal structure reminiscent of prior liquation. Note also that a significant amount of liquation apparently occurred along several of the segregation bands and that grain boundaries appear to be pinned at these locations. Further note that the average grain size observable in Fig. 8 is essentially identical to that shown previously in Fig. 7. This observation, together with the fact that

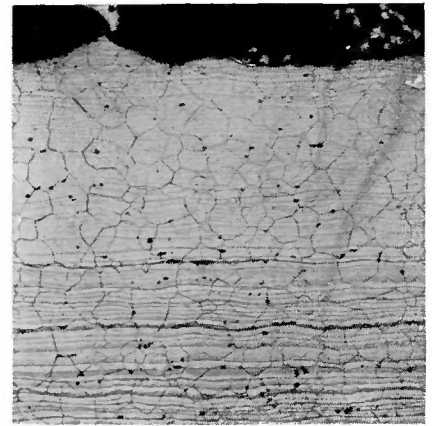


Fig. 6—Microstructure produced in as-received material heated at 1000° F/sec to 2200° F and immediately water quenched. 10% chromic acid electrolytic etch followed by 10% ferric chloride etch. X100 (reduced 28% on reproduction)



Fig. 7—Microstructure produced in as-received material heated to 2350° F in 2.2 sec and immediately water quenched. 10% chromic acid electrolytic etch followed by 10% ferric chloride etch. X100 (reduced 28% on reproduction)

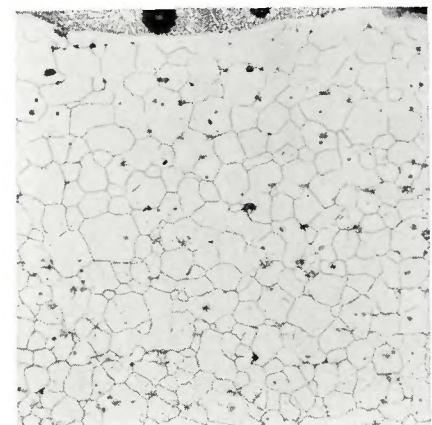


Fig. 8—Microstructure produced in as-received material heated to 2400° F in 2.2 sec and immediately water quenched. 10% chromic acid electrolytic etch followed by 10% ferric chloride etch. X100 (reduced 28% on reproduction)

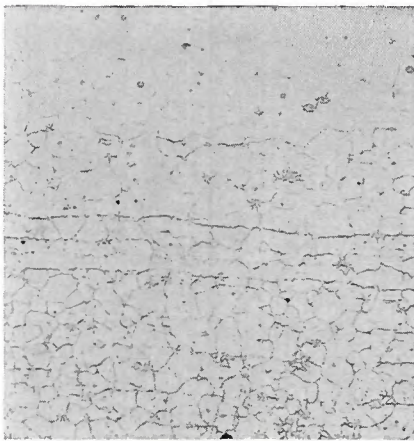


Fig. 9—Microstructure produced in as-received material heated to 2450° F in 2.2 sec and immediately water quenched. 10% chromic acid electrolytic etch followed by 10% ferric chloride etch. X100 (reduced 28% on reproduction)

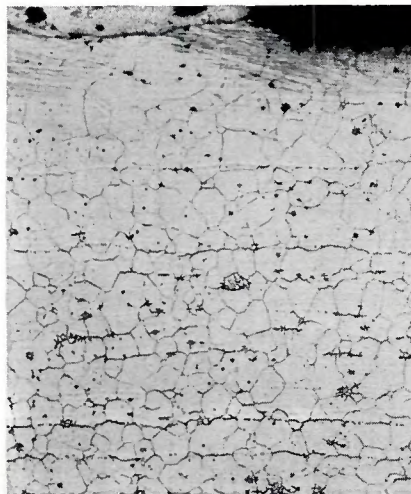


Fig. 10—Microstructure produced in as-received material heated to 2500° F in 2.2 sec and immediately water quenched. 10% chromic acid electrolytic etch followed by 10% ferric chloride etch. X100 (reduced 28% on reproduction)

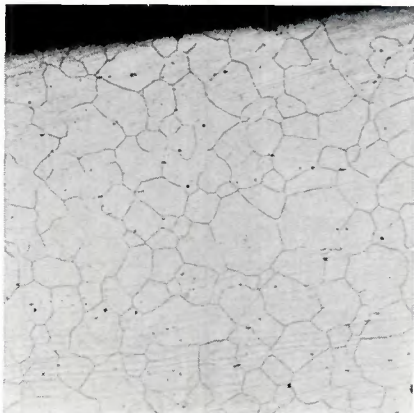


Fig. 11—Microstructure produced in as-received material heated to 2350° F in 2.2 sec, held at 2350° F for 1 sec and immediately water quenched. 10% chromic acid electrolytic etch followed by 10% ferric chloride etch. X100 (reduced 28% on reproduction)

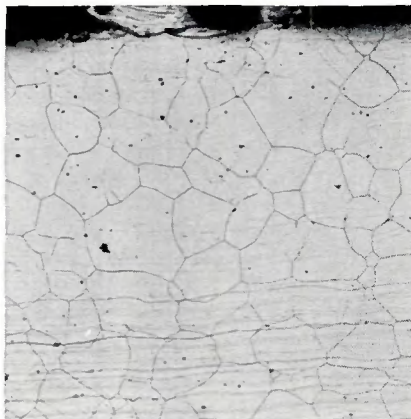


Fig. 12—Microstructure produced in as-received material heated to 2350° F in 2.2 sec, held at 2350° F for 3 sec and immediately water quenched. 10% chromic acid electrolytic etch followed by 10% ferric chloride etch. X100 (reduced 28% on reproduction)

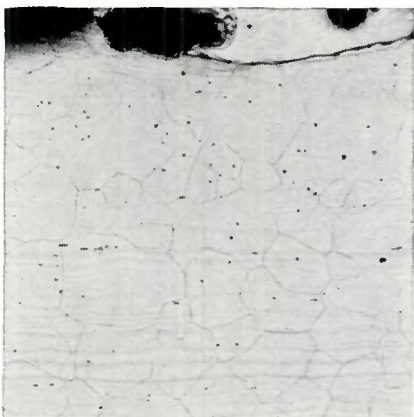


Fig. 13—Microstructure produced in as-received material heated to 2350° F in 2.2 sec, held at 2350° F for 6 sec and immediately water quenched. 10% chromic acid electrolytic etch followed by 10% ferric chloride etch. X100 (reduced 28% on reproduction)

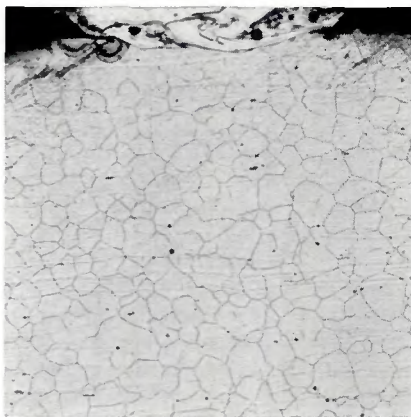


Fig. 14—Microstructure produced in as-received material heated to 2350° F in 2.2 sec, held at 2350° F for 12 sec and immediately water quenched. 10% chromic acid electrolytic etch followed by 10% ferric chloride etch. X100 (reduced 28% on reproduction)

many of the grain boundaries are associated with liquated pools, suggest that solute-rich liquid originating in the “constitutionally liquated” pools penetrated the grain boundaries and prevented normal grain growth.

Figures 9 and 10 are photomicrographs at X100 showing the structures formed by rapid heating at 2450 and 2500° F, respectively, and immediately quenching to room temperature. The fact that the microstructure in both cases is essentially identical to that observed in Fig. 8 clearly establishes:

1. That a liquid grain-boundary film definitely forms at temperatures significantly below the equilibrium solidus of the alloy.

2. The presence of the liquid grain-boundary film definitely inhibits the grain-boundary migration associated with normal growth.

*Holding at Peak Temperature.* The previous section established that “constitutional liquation” is the probable mechanism responsible for inhibiting normal grain-boundary migration during rapid heating to temperatures above 2400° F. However, if the formation of a liquid grain-boundary film formed by “constitutional liquation” of titanium-sulfide inclusions is responsible for inhibiting normal grain-boundary motion at temperatures above 2400° F, normal grain growth would be expected at temperatures below 2400° F. Furthermore, normal grain growth should resume after exposure to temperatures above 2400° F to eliminate the liquid grain-boundary films formed by “constitutional liquation” by diffusion of solute to the matrix in accordance with the theory presented in the previous paper.<sup>1</sup> In order to check the validity of the theory in this regard, the following series of experiments were conducted.

Peak temperatures of 2350, 2400, 2450, and 2500° F were selected for investigation. One specimen was heated to each of the above temperatures in 2.2 sec, quenched to room temperature immediately, and examined metallographically. Additional specimens were heated to each of the four peak temperatures in 2.2 sec, held at temperature for 1, 3, 6 and 12 sec, quenched to room temperature and examined metallographically.

Figures 7 and 11–14 show the microstructures produced by heating to 2350° F in 2.2 sec and holding isothermally for 0, 1, 3, 6 and 12 sec, respectively. It should be noted that at 2350° F, where no “constitutional liquation” was observed, normal grain growth began immediately and the grain size increased continuously with increase in the time of exposure.

It should be mentioned at this point that a temperature gradient was known to be present in these specimens. However, in each figure, the control thermocouple was located at the top-center portion of the field of view and an accurate record of the temperature in the vicinity of this point was obtained in every case. Therefore, in these and all subsequent figures in this section, the microstructure located within 2 in. (at X100 magnification) of the thermocouple location should be taken as representative and all comparisons made on this basis.

Figures 8 and 15-18 show the microstructures produced by heating to 2400° M in 2.2 sec and holding isothermally for 0, 1, 3, 6 and 12 sec, respectively. Note that the evidence of scattered "constitutional liquation" produced immediately upon reaching 2400° F (Fig. 8) is completely absent and that normal grain growth has already begun in the specimen held 1 sec at 2400° F (Fig. 15). With reference to Figs. 16-18 (held at 2400° F for 3, 6 and 12 sec, respectively), it is obvious that the grain size increases continuously with increase in the time of exposure to 2400° F.

Figures 9 and 19-22 show the microstructures produced by heating to 2450° F in 2.2 sec and holding for 0, 1, 3, 6 and 12 sec, respectively. Note that evidence of scattered "constitutional liquation" is observed in the specimen heated to 2450° F (Fig. 9) and immediately quenched to room temperature. A slight increase in grain size is noted in Figs. 19 and 20 (held at 2450° F for 1 and 3 sec, respectively). However, the grain boundaries are associated with remnants of "constitutional liquation," suggesting that normal grain growth has been slowed to some degree. Figures 21 and 22 (held at 2450° F for 6 and 12 sec, respectively) show no evidence of "constitutional liquation" or grain-boundary pinning, but do show a rapid continuous increase in grain size with increasing time of exposure to 2450° F.

Figures 10 and 23-26 show the microstructures produced by heating to 2500° F in 2.2 sec and holding for 0, 1, 3, 6 and 12 sec, respectively. Note that most grains in Figs. 10, 23 and 24 (held 0, 1 and 3 sec, respectively) show evidence of a nearly continuous liquid network along the grain boundaries. Note also that no significant change in grain size is evident in any of these figures as compared to the recrystallized grains in Fig. 6. However, after 6 sec at 2500° F (Fig. 25) the grain size had increased significantly and evidence of liquid films was

confined primarily to isolated triple points between adjacent grains. After 12 sec at 2500° F (Fig. 26), the grain size further increased and no evidence of the liquated films remained.

The average grain diameter  $D$  of each of the 20 specimens described above was determined by standard statistical techniques.<sup>3</sup> These data are summarized in Fig. 27. Note that the square of the average grain diameter is plotted as a function of  $t$ , the time of exposure to peak temperature, for each of the four temperatures discussed above.

Referring to Fig. 27, it can be seen that square of the average grain diameter appears to increase as a linear function of the time of exposure at 2350 and 2400° F, as would be expected for normal grain-growth. However, at 2450 and 2500° F, the beginning of normal growth appears to be delayed for periods of approximately

3 and 6 sec, respectively. These times correspond to the times required to eliminate all evidence of grain boundary liquation by diffusion at these temperatures as discussed previously in connection with the foregoing photomicrographs.

Once normal growth was initiated at these temperatures, however, the growth rate again appeared to increase as the temperature was increased. Thus, the slope of each of the four curves,  $D^2/t$ , was determined for the region of normal growth and the logarithms of these values were plotted as a function of the reciprocal of absolute temperature in Fig. 28. Although some scatter is evident, a reasonable correlation is provided by the straight line which was drawn to correspond to the activation energy of 68 Kcal/g atom reported<sup>4</sup> for self diffusion in  $\gamma$ -iron.

Thus, it appears that normal grain

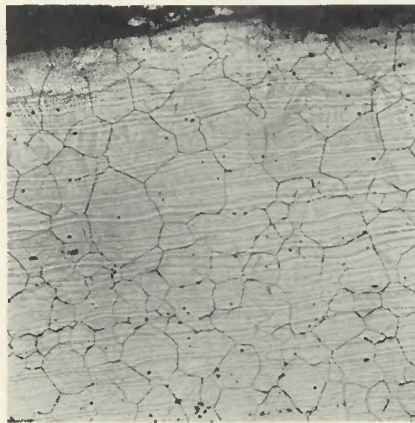


Fig. 15—Microstructure produced in as-received material heated to 2400° F in 2.2 sec, held at 2400° F for 1 sec and immediately water quenched. 10% chromic acid electrolytic etch followed by 10% ferric chloride etch. X100 (reduced 28% on reproduction)

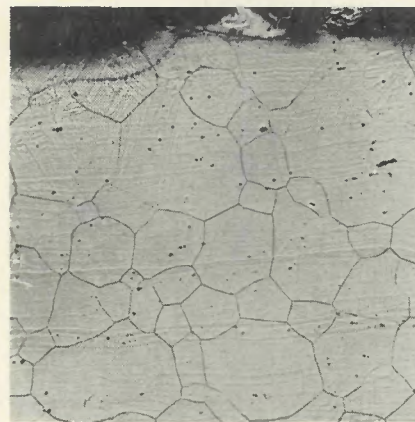


Fig. 17—Microstructure produced in as-received material heated to 2400° F in 2.2 sec, held at 2400° F for 6 sec and immediately water quenched. 10% chromic acid electrolytic etch followed by 10% ferric chloride etch. X100 (reproduced 28% on reproduction)

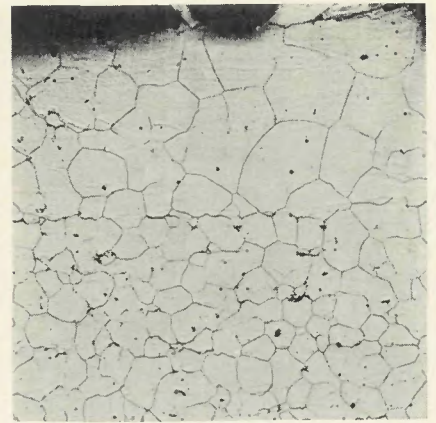


Fig. 16—Microstructure produced in as-received material heated to 2400° F in 2.2 sec, held at 2400° F for 3 sec and immediately water quenched. 10% chromic acid electrolytic etch followed by 10% ferric chloride etch. X100 (reduced 28% on reproduction)

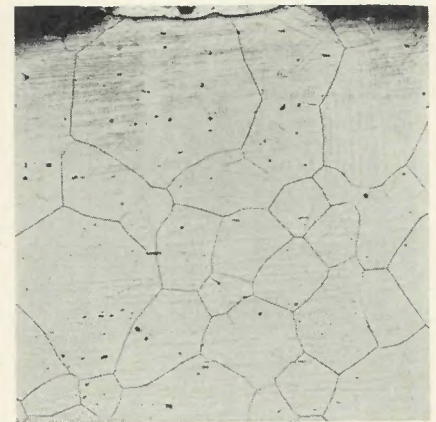


Fig. 18—Microstructure produced in as-received material heated to 2400° F in 2.2 sec, held at 2400° F for 12 sec and immediately water quenched. 10% chromic acid electrolytic etch followed by 10% ferric chloride etch. X100 (reduced 28% on reproduction)

growth was inhibited in all specimens exhibiting evidence of "constitutional liquation" and that normal grain growth resumed as soon as all evidence of grain-boundary liquation disappeared during isothermal exposure to peak temperature. Therefore, the anomalous grain size distribution observed in weld heat-affected zone of 18 Ni maraging steels can be attributed to normal grain-boundary migration being inhibited by a liquid grain-boundary film resulting from "constitutional liquation" of titanium-sulfide inclusions at temperatures above 2400° F. A larger grain size is observed in regions of the weld heat-affected zone experiencing lower peak temperatures because normal grain growth continues in these regions while at the same time normal grain growth is inhibited by liquid grain-boundary films in regions of the weld heat-affected zone experiencing peak

temperatures greater than 2400° F.

*Gas Tungsten-Arc Weld in 1/2 in. Plate.* Figure 29 shows a portion of the top surface on the bead-on-plate gas tungsten-arc weld deposited on 1/2 in. 18 Ni maraging steel as revealed by a nital etch at X50 magnification. The original photomicrographs were re-photographed at approximately X1/3. The dark etching region of the fusion zone delineates the final "crater" produced by abruptly interrupting the arc current. The sudden elimination of the arc as a heat source near the center of the weld puddle permitted a rapid increase in the rate of growth at the solid-liquid interface, thus causing a marked decrease in the dimensions of the subgrains produced during solidification of the terminal crater.

The tapered, lighter etching band within the fusion zone, immediately adjacent to the fusion line is represen-

tative of solidification substructure at the rear of the moving weld puddle. The width of this band decreases to zero at point A, located near the right hand edge of Fig. 29 at a position corresponding to the widest point of the weld puddle at the time of interruption of the arc current.

Figure 30 represents the structure in the vicinity of the fusion line along the leading edge of the solidified weld crater as revealed by a nital etch at X250 magnification. The epitaxial relationship between adjacent regions on opposite sides of the fusion line is clearly evident from the contiguous nature of the grain boundaries and the differently oriented solidification substructure within each grain of the solidified weld metal.

It should also be noted that the heat-affected zone grain boundaries immediately adjacent to the fusion line appear to be more heavily etched than grain boundaries further from the fusion line. This can be readily explained if one assumes that the boundaries adjacent to the fusion zone are enriched in solute, thus making them more susceptible to chemical attack by the etchant. Canonico<sup>5</sup> has reported, as a result of electron microprobe analysis, that grain boundaries in 18 Ni maraging steel exhibiting this characteristic are rich in titanium. Unfortunately, he did not analyze for other elements.

Attention is also drawn to the small, irregularly shaped, grey regions located within some of the grains in the heat-affected zone immediately adjacent to the fusion line. These regions are produced by "constitutional liquation" of second-phase particles.

Note that no evidence of either dark etching grain boundaries or "constitutional liquation" is present at a distance greater than approximately 0.0025 in. (0.625 in. at X250) from the fusion line. This is indicative of the fact that the distribution of peak temperatures at the leading edge of the weld puddle was extremely steep so that the peak temperature necessary to produce these phenomena was only experienced within 0.0025 in. of the leading edge of the weld puddle.

Figure 31 shows the microstructure in the immediate vicinity of the letter A in Fig. 29 as revealed by a nital etch at X250 magnification. Two very interesting microstructural features can be seen within the heat-affected zone in this photomicrograph. First, note the "ghost" grain boundaries which appear as a series of surface irregularities paralleling the grain boundaries, suggesting that these particular boundaries experienced melting

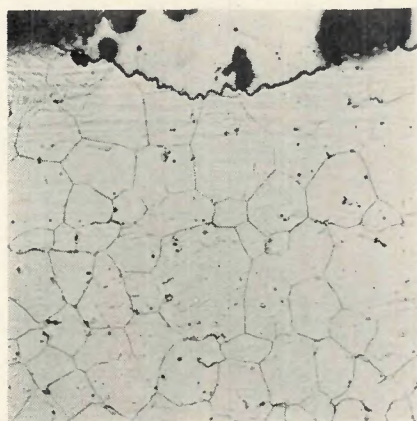


Fig. 19—Microstructure produced in as-received material heated to 2450° F in 2.2 sec, held at 2450° F for 1 sec and immediately water quenched. 10% chromic acid electrolytic etch followed by 10% ferric chloride etch. X100 (reduced 28% on reproduction)

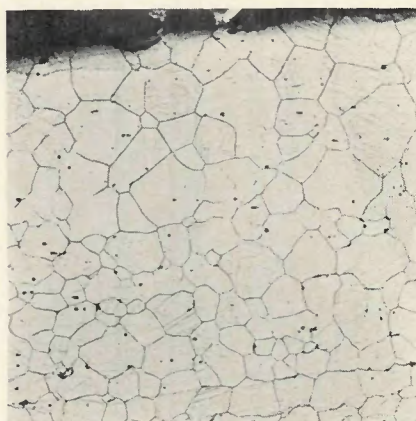


Fig. 20—Microstructure produced in as-received material heated to 2450° F in 2.2 sec, held at 2450° F for 3 sec and immediately water quenched. 10% chromic acid electrolytic etch followed by 10% ferric chloride etch. X100 (reduced 28% on reproduction)



Fig. 21—Microstructure produced in as-received material heated to 2450° F in 2.2 sec, held at 2450° F for 6 sec and immediately water quenched. 10% chromic acid electrolytic etch followed by 10% ferric chloride etch. X100 (reduced 28% on reproduction)



Fig. 22—Microstructure produced in as-received material heated to 2450° F in 2.2 sec, held at 2450° F for 12 sec and immediately water quenched. 10% chromic acid electrolytic etch followed by 10% ferric chloride etch. X100 (reduced 28% on reproduction)

and progressive solidification. In addition, note that the narrow dark etching grain boundaries produced during subsequent allotropic transformation appear to be located at one edge of the wide parallel bands referred to as "ghost" boundaries.

Careful examination of Fig. 29 reveals that the instantaneous location of the solid-liquid interface, at the time of arc cut-off, was tangent to the weld heat-affected zone in this region. Further examination reveals that the "ghost" grain boundaries become less pronounced at the right side of Fig. 29, where the time of exposure to peak temperature sufficiently high to produce "constitutional liquation" and grain boundary migration was relatively short. That is to say, the closer one approaches the center of the leading edge of the weld puddle, the more rapid is the rate of heating and cooling and the shorter is the time of exposure to a particular peak temperature. Therefore, the extent to which an activated process proceeds is less at the leading edge of the weld puddle than at the side or the rear of the weld puddle.

The other important feature visible in Fig. 31 is the evidence of a metallurgical reaction between certain types of second-phase particles and the matrix. The morphology of these areas is identical to that proposed by Dudley<sup>6</sup> in his "constitutional liquation" hypothesis. Attention is drawn to the relatively large elliptical-shaped region slightly to the left and below the center of Fig. 31. Note that remnants of the original second-phase particle are visible near the center of the grey-etching reaction product.

Figure 32 is a photograph at X250 magnification just outside the field of view at the left edge of Fig. 29. Note that the dark etching boundaries produced during subsequent allotropic transformation are still associated with the so-called "ghost" boundaries. Also note that no evidence of "constitutional liquation" is present. This suggests that in this region of the heat-affected zone, sufficient time was available at elevated temperatures to completely dissipate all evidence of this phenomenon except that provided by the etching behavior of the "ghost" boundaries.

The portion of the gas tungsten-arc weld bead on 1/2 in. plate shown in Fig. 33 was located considerably behind the location of the terminal crater. Note that the narrow, dark-etching grain boundaries resulting from allotropic transformation during cooling are no longer associated with the "ghost" boundaries in this region. It is postulated that the relatively long time

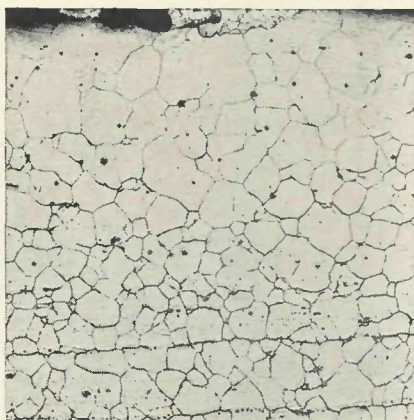


Fig. 23—Microstructure produced in as-received material heated to 2500° F in 2.2 sec, held at 2500° F for 1 sec and immediately water quenched. 10% chromic acid electrolytic etch followed by 10% ferric chloride etch. X100 (reduced 28% on reproduction)

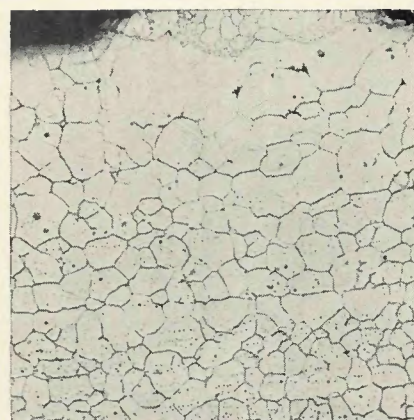


Fig. 24—Microstructure produced in as-received material heated to 2500° F in 2.2 sec, held at 2500° F for 3 sec and immediately water quenched. 10% chromic acid electrolytic etch followed by 10% ferric chloride etch. X100 (reduced 28% on reproduction)

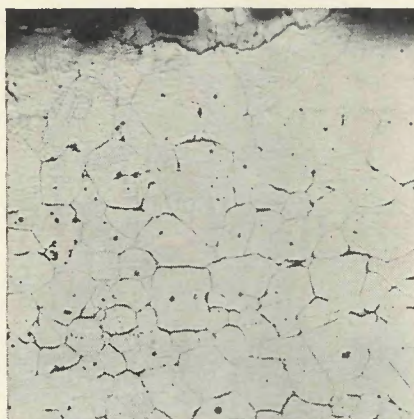


Fig. 25—Microstructure produced in as-received material heated to 2500° F in 2.2 sec, held at 2500° F for 6 sec and immediately water quenched. 10% chromic acid electrolytic etch followed by 10% ferric chloride etch. X100 (reduced 28% on reproduction)

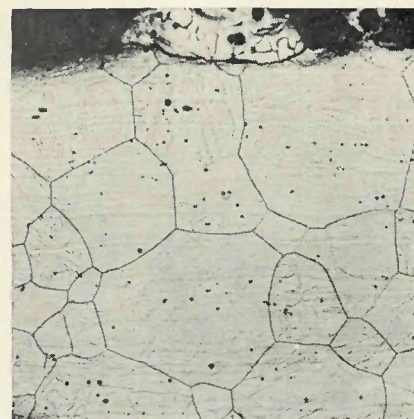


Fig. 26—Microstructure produced in as-received material heated to 2500° F in 2.2 sec, held at 2500° F for 12 sec and immediately water quenched. 10% chromic acid electrolytic etch followed by 10% ferric chloride etch. X100 (reduced 28% on reproduction)

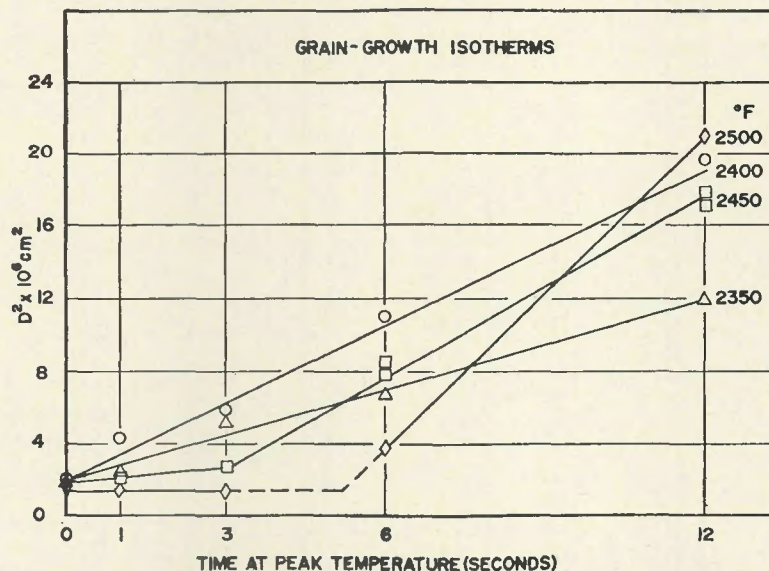


Fig. 27—Plot of the square of the average grain diameter as a function of time of exposure to peak temperatures of 2350, 2400, 2450 and 2500° F

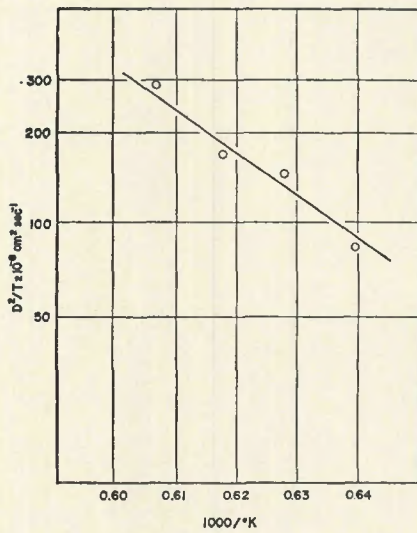


Fig. 28—Plot of log rate of grain growth as a function of reciprocal temperature

of exposure to temperatures near the peak of the weld thermal cycle experienced at this location was sufficient to permit the actual grain boundaries to break away from the solute-rich "ghost" boundary regions.

Once the actual grain boundaries escape the solute-rich regions, further migration can occur readily until either the instantaneous temperature falls below the effective coarsening

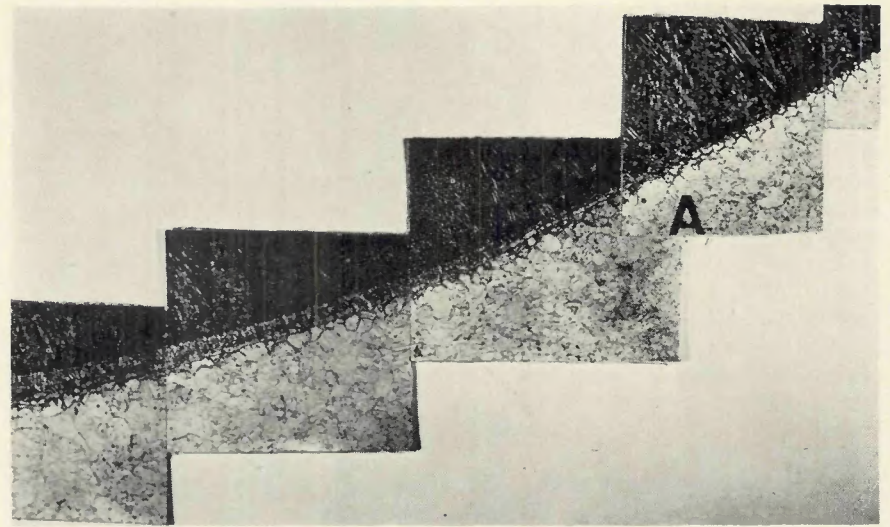


Fig. 29—Microstructure of the top surface of a gas tungsten-arc weld bead on 1/2 in. plate. X50 (reduced 2/3 by re-photographing original photomicrographs), nital etch

temperature or an equilibrium grain boundary network is established. Thus, the narrow dark-etching transformation grain boundaries in Fig. 33 probably conform more closely to an equilibrium grain boundary network than would be the case had they remained associated to the solute-rich "ghost" boundaries.

A schematic representation of grain boundary movement near the fusion

line of a typical weldment experiencing "constitutional liquation" is shown in Fig. 34.

Figure 34A illustrates the instantaneous temperature distribution along the line A'-A at the instant the moving arc is located as shown. The microstructure at location  $d_0$  (Fig. 34B), which is sufficiently removed from the molten weld pool to be unaffected by the heat of welding, can be taken as representative of the as-received plate. Figure 34B also shows, in schematic fashion, the microstructure that would exist at location  $d_1$ . Note that at this location significant grain growth has occurred due to the heat of welding. Note also, that concurrent with grain growth, the temperature is sufficiently high to initiate "constitutional liquation" and that some solute-rich liquid has penetrated the grain boundaries. At a location  $d_2$  slightly to the right of location  $d_1$  sufficient solute-rich liquid would be expected to penetrate the grain boundaries to inhibit further grain boundary migration. No further grain growth would be expected until either the solute-rich liquid phase was dissipated by homogenization or until the instantaneous temperature decreased below the effective solidus of the solute-rich liquid.

If insufficient time were available to dissipate the liquid grain-boundary film before the instantaneous temperature decreased to below the effective solidus of the liquid, grain boundary movement would begin almost immediately and a solute-rich "ghost" grain boundary network would remain fixed. Grain growth would continue until either an equilibrium grain-boundary network was formed or the temperature decreased to below the effective coarsening temperature of



Fig. 30—Microstructure along the fusion line of the top surface of a gas tungsten-arc weld bead on 1/2 in. plate. Nital etch. X250 (reduced 50% on reproduction)

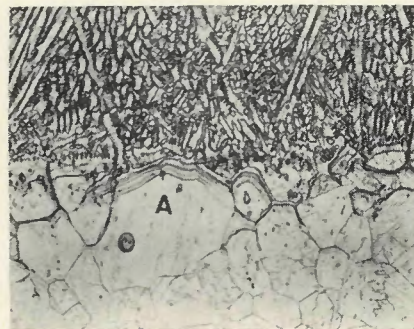


Fig. 31—Microstructure along the fusion line of the top surface of a gas tungsten-arc weld bead on 1/2 in. plate. Nital etch. X250 (reduced 50% on reproduction)

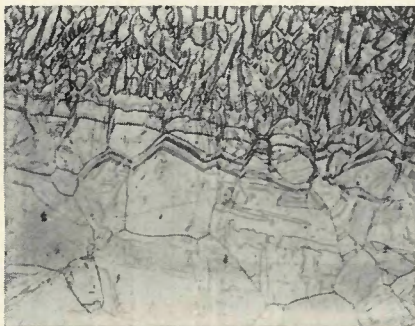


Fig. 32—Microstructure along the fusion line of the top surface of a gas tungsten-arc weld bead on 1/2 in. plate. Nital etch. X250 (reduced 50% of reproduction)

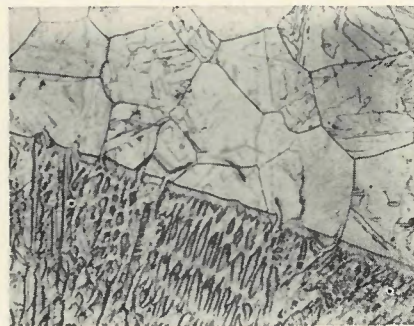


Fig. 33—Microstructure along the fusion line of the top surface of a gas tungsten-arc weld bead on 1/2 in. plate. Nital etch. X250 (reduced 50% on reproduction)

the alloy. Thus, at room temperature, location  $d_3$ , both the real grain boundaries and the solute-rich "ghost" networks would be visible in the microstructure.

The aforementioned discussion of grain boundary movement near the fusion line of a typical weldment experiencing "constitutional liquation" is completely consistent with the observations noted near the fusion line of 18 Ni maraging steel weldments.

## Conclusions

The following conclusions pertain to the studies of typical fusion weldments:

1. The grain size in the weld heat-affected zone in an 18 Ni maraging steel immediately adjacent to the weld fusion line was observed to be significantly smaller than the grain size further removed from the weld fusion line.

2. Evidence of "constitutional liquation" and grain boundary segregation was observed in the weld heat-affected zone near the terminal weld crater immediately adjacent to the weld fusion line. However, no evidence of "constitutional liquation" was observed in the weld heat-affected zone immediately adjacent to the fusion line at locations considerably behind the trailing edge of the terminal crater.

3. In regions of the weld heat-affected zone immediately adjacent to the weld fusion line and considerably behind the trailing edge of the terminal crater, evidence of "ghost" grain boundaries was evident.

The following conclusions pertain to the Gleeble studies:

1. All specimens heated to peak temperatures below that necessary to produce "constitutional liquation" exhibited normal grain growth during isothermal exposure at peak temperature.

2. Normal grain growth was inhibited by a liquid grain-boundary film in all specimens heated to peak temperatures above that necessary to produce "constitutional liquation" and quenched immediately. Normal grain growth resumed as soon as all evidence of the liquid grain boundary film disappeared during isothermal exposure to these peak temperatures.

3. Plots of the square of the grain diameter vs. time of exposure to peak temperature proved to be straight lines for temperatures of 2350 and 2400° F which did not cause "consti-

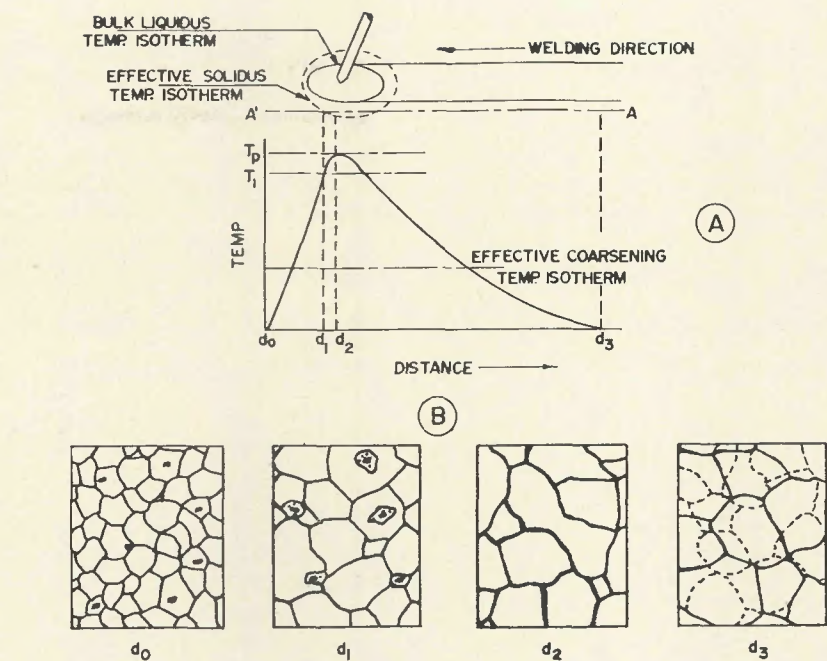


Fig. 34—Schematic representation of grain boundary movement in a hypothetical weld heat-affected zone along line A-A

tutional liquation."

4. Plots of the square of the grain diameter vs. time of exposure to temperatures of 2450 and 2500° F, which caused "constitutional liquation," showed that no significant change in grain size occurred until after exposure to the test temperature for a sufficient time to dissipate the grain boundary films by diffusion.

5. The anomalous grain size distribution observed in the weld heat-affected zone, immediately adjacent the fusion line, of the 18 Ni maraging steels was attributed to grain boundary pinning by a liquid film produced by "constitutional liquation" of titanium sulfide inclusions.

The following conclusions pertain to the "ghost" boundary studies:

1. The "ghost" boundary structure was produced because of incomplete homogenization of the solute-rich grain boundary film produced by "constitutional liquation" of titanium sulfide inclusions.

2. The sequence of events leading up to the formation of the "ghost" boundary networks are:

(a) As a result of the heat of the advancing weld puddle, normal grain growth proceeds until the temperature in the heat-affected zone is sufficiently high to initiate "constitutional liquation."

(b) The moving grain boundaries then intercept the solute-rich liquid pools caused by "constitutional liqua-

tion" and are pinned due to the wetting action of the solute-rich liquid.

(c) Continued movement of the weld puddle causes the temperature in the heat-affected zone to decrease, causing the solute-rich liquid grain boundary film to solidify. At this instant in time, the high angle grain boundaries are freed and continue to move until either the temperature of the heat-affected zone decreases below the effective coarsening temperature or a equilibrium grain boundary network is established.

(d) The solute-rich regions associated with the previously liquated grain boundaries remain fixed and are revealed by the solute sensitive etchant to be separate and distinct from the normal high angle grain boundaries in many areas.

## References

1. Pepe, J. J., and Savage, W. F., "Effects of Constitutional Liquation in 18 Ni Maraging Steels," WELDING JOURNAL, 46 (9), Research Suppl., 411-s to 422-s (1967)
2. Decker, R. F., "Maraging Steels; Structure-Property Relations," Proceeding of Symposium, "Relations Between the Structure and Mechanical Properties of Metals," National Physical Laboratory, Teddington, England (January 1963)
3. Hilliard, J. E., "Grain Size Estimation," G. E. Research Lab. No. 62-RL-3133M, Dec. 1962
4. Smithells, C. J., Metals Reference Book, V2, 3rd Edition, Butterworths, Washington (1962)
5. Canonico, D. A., Private Communication
6. Dudley, R. H., "An Experimental Investigation of the Constitutional Liquation Hypothesis," Ph.D. Thesis, Rensselaer Polytechnic Institute, January 1962